

# Wave heave sensor verification in dry conditions with optoelectronic reference

Mohamad Khalil<sup>1</sup>, Francesco Crenna<sup>1</sup>, Giovanni Battista Rossi<sup>1</sup>

<sup>1</sup> Department of Mechanical, Energy, Management and Transport Engineering (DIME), University of Genoa, Italy

## ABSTRACT

Sea state information is required for coastal engineering and safety of navigation. Inertial Measurement Units (IMUs) are playing an effective role in the estimation of the sea state in real time application also. In this paper, a novel method for heave inertial sensors verification in a dry environment is presented. The main peculiarity is that the IMU movement is measured through an optoelectronic external instrument, and not guaranteed by the mechanical assembly of the movement generation device. Furthermore, the generated movement presents reality aspects, such as oscillations of the sensors, that are not common in similar devices. The proposed approach has been tested considering a general purpose IMU, which requires a processing procedure to measure the heave. Two possible procedures based on different filtering approaches are proposed and compared. The test procedure enables a quantitative evaluation of the heave measurement by inertial sensors including the evaluation of measurement uncertainty in each test conditions.

Section: RESEARCH PAPER

Keywords: IMU; buoys calibration; wave spectrum; heave measurement

Citation: M. Khalil, F. Crenna, G. B. Rossi, Wave heave sensor verification in dry conditions with optoelectronic reference, Acta IMEKO, vol. 13 (2024) no. 4, pp. 1-10. DOI: [10.21014/actaimeko.v13i4.1768](https://doi.org/10.21014/actaimeko.v13i4.1768)

Section Editor: Andrea Scorza, Università degli Studi Roma Tre, Italy

Received February 8, 2024; In final form August 12, 2024; Published December 2024

Copyright: This is an open-access article distributed under the terms of the Creative Commons Attribution 3.0 License, which permits unrestricted use, distribution, and reproduction in any medium, provided the original author and source are credited.

Funding: Work supported by European Union – Next Generation EU and funded by the Ministry of University and Research (MUR), National Recovery and Resilience Plan (NRRP), Mission 4, Component 2, Investment 1.5, project “RAISE – Robotics and AI for Socio-economic Empowerment” (ECS00000035).

Corresponding author: Mohamad Khalil, e-mail: [mohamad.khalil01@edu.unige.it](mailto:mohamad.khalil01@edu.unige.it)

## 1. INTRODUCTION

Nowadays, sea wave measurements are mainly carried out locally by dedicated buoys (moored or drifting) [1]. Wave buoys are typically constructed with a spherical geometry and have small size to better follow the water movement; thanks to their design, they play an effective role in following the ocean circulation and surface topography variation over time. Meteorological buoys, however, can measure weather parameters through various sensors, including wave and wind sensors, thermometers, Global Navigation Satellite System (GNSS) receiver and others, but are less optimised for wave measurement. Concerning waves, raw signals describe the buoy movements and can be processed onboard to obtain wave information, sea state estimation and directional spectra measured at the buoy mooring location.

Buoys rely on a communication system, or radio transmission, to send data to onshore monitoring stations. Such transmissions affect the buoy power consumption and data transmission is limited by the available bandwidth. For these reasons, the buoy usually transmits data packages for a certain amount of time and

then it turns in standby mode for a period. This procedure, although advantageous for power management, may present some issues when sea state is rapidly changing. In such conditions, transmission would improve sea state estimation and forecast of met-ocean conditions. Moreover, often rapidly changing conditions present rather large spatial variations, so a dense buoys distribution would be required for optimal sea monitoring, especially in critical coastal areas.

In this scenario, the National Recovery Program (NRP) has constituted the Robotics and AI for Socio-economic Empowerment innovation ecosystem, RAISE. One of RAISE’s areas concerns ports activities and includes a research project concerning nowcasting and forecasting of met-ocean conditions. The main goals are the monitoring and the prevention of risks for navigation and coastal environments, by suited protection technologies. To pursue these goals, several research activities are foreseen, including both the development of a new sea-wave measurement method, of special interest here, to overcome some of the issues connected to buoy-based wave measurements, and considering new approaches to estimate the sea state [2].

The aim of this research project is to enable small vessels navigating near the harbour to act as potential moving measurement systems, to monitor waves and sea state in different locations. Therefore, these vessels should be properly equipped to measure their own motion, and appropriate procedures for indirectly measuring the sea state based on these observations should be implemented, with real-time responses. This kind of indirect measurement of sea state often called “the wave buoy analogy”, involves the solution of a complex dynamics-inversion problem. For practical application, issues such as the reliability of the solution and the calculation time – since real time application is highly desirable – should also be accounted for. Thus, different solutions have been considered, especially in the last, say, twenty years, and research in this subject is still ongoing. Basically, frequency domain [3] and time domain approaches [3], [4] have been investigated, and a few experimental validations have also been carried out [5], [6]. Yet, metrological issues concerning the reliability and the uncertainty of the inertial measurement, which constitutes the starting point of the process, and thus whose quality strongly affects the results, seem to have not been explicitly considered in the aforementioned, though fundamental, studies. This consideration led to the motivation for the present study, which focuses on addressing these issues.

The goal is to develop an affordable wave measurement system that can be deployed onboard small vessels. This system would utilize IMUs, which can be integrated with a GNSS antenna, to accurately measure vessel motion and orientation. Today, Micro-Electro-Mechanical System (MEMS) based IMU are used for sea surface wave measurements [7]. On the market, there are some, IMU based, ready-out-of-the-box heave measurement systems, but their application is limited to large vessels or specific marine applications [8], [9]. In general, when using an IMU, some measurement problems arise, due for example to sensors’ offset, offset drift and magnetic interference. Therefore, if IMUs not specialized for heave measurements must be used, it is recommended to verify their performance. Metrological verification procedures are fundamental for measurement quality assessment in general [10], and especially in this case, where the sensor-plus-processing combination must be verified.

Sensors for sea wave movements can be verified in wet or in dry conditions. Wet verification requires a controllable, reliable, wave generator. Some setups can be found in the literature [11], [12], the most common being a wave tank or flume of proper length and transverse dimensions, to create open-sea conditions. Water movement is measured by video cameras, underwater cameras, and wave gauge, and the buoy itself, or the sensor is placed inside the testing section on a floating body. Dry conditions are more suitable for laboratory testing and offer a wide range of possibilities for reference movement generation and measurement. The literature is rather sparse regarding dry calibration setups. For example, Datawell BV seems to be the main reference [13]. They proposed a calibration method for their buoys in dry conditions, by using two ways for generating wave motion [14]. The first one is an active pendulum setup, with two controlled motors. The main motor operates on the centre of rotation of the system, while the second acts on the buoy support. The motors are controlled to work synchronously, in such a way that the system under test is kept aligned with the earth gravity direction during the movement. The second technique is much simpler: the buoy is attached to a high ceiling with a rope, to create a free pendulum. This second option,

although simpler, is less flexible and it is difficult to closely control and vary the relevant parameters. In fact, the vertical axis inclination of the buoy accelerometer must be considered, since during the buoy movement the vertical axis is not aligned toward the earth gravity. Yet the controlling procedure seems to be somewhat uncertain, since it depends on a ruler and on the eye vision, to detect the vertical displacement of the buoy.

Another dry test facility is described in [15] and operates at the National Centre of Ocean Standards and Metrology, China. In this case, the wave dry simulator is based on a large wheel, on which the buoy or the heave measurement system under test is installed. The wheel rotation, controlled by a motor, allows simulation of sea waves heights ranging from 1 m to 6 m, depending on the mounting position on the wheel, with periods from 2 s to 40 s, depending on motor control parameters. A particularity of this calibration device is that it allows the simulation of the typical orbital movements of the buoy when influenced by the sea waves.

It is worth noting that such test setups are focused on the vertical movement of the system under test. When dealing with sea state estimation, it is necessary to verify the overall measurement chain for the displacements and the processing required to estimate the sea state. In these cases, the reproduction of the movement along a wave slope is required. The work [16] proposes a mechanical setup able to create a biaxial angular motion of the buoy with amplitudes  $15^\circ$  and  $25^\circ$  and a vertical motion up to 0.45 m. A ferry-like wheel with a controlled rotation axis is considered in [17] to simulate wave slope movement.

A new technology, the Datawell DWR-GPS wave buoy, is introduced for measuring sea state parameters, based on an integrated GNSS receiver. To validate these new buoys, field experiments are required, using a reference system such as the accelerometer based Datawell DWR buoy. The study shows a new valuable instrument to the ocean wave measuring community [18]. Other research projects investigate the validation of GNSS-based buoys for measuring sea state, using both dry and wet tests [19], [20], respectively. The dry test involves installing a GNSS receiver on a pendulum controlled by a motor at the centre of rotation, with the receiver holder freely aligned with Earth's gravity. The first reference involves wave periods ranging from 6 to 10 seconds, while the second reference involves a range from 11 to 15 seconds. The wet test involves installing the GNSS receiver on a moored GNSS buoy, and the studies show that the output velocity signal of the receiver is reasonable for ocean wave measurements.

To carry out a calibration or even a sensor verification, it is necessary to have a known controllable input or, in this case, a vertical movement of the device under test. To this purpose, all the dry experiments found in the literature are based on developing very precise mechanical architectures and on trusting the mechanical equipment, which is regarded as the reference displacement sample.

In the present study, the proposed setup tries to incorporate the advantages of the literature experiments while adding some flexibility. The double-axis pendulum setup is maintained, but now with only one controlled axis, while the second is free and creates oscillations of the sensor stand due to its inertia. The sensor under test does not move perfectly aligned in the horizontal plane; rather, an additional angular movement is introduced, simulating the small movement along the wave slope or the slight angular oscillations due to vessel motion in a real application. Furthermore, the verification is based on an external

optoelectronic reference instrument, so it does not rely entirely on the mechanical accuracy of the movement device.

This approach has been applied to a general-purpose IMU. Raw signals are acquired and then processed to obtain the vertical displacement, since the sensor does not have an internal processing for sea wave measurement. Two alternative processing techniques have been evaluated, and results are compared with the heave accuracy specification for a commercial IMU wave sensor.

The paper is organized as follows. Section 2 recalls some details regarding heave measurement by Inertial Measurement Units and highlights the problems to be faced. Section 3 presents the experimental setup, including the calibration device, the reference instrument, and the sensor under test. Section 4 describes the data processing required to obtain the heave measurement and the method used to compare IMU results with the reference. Section 5 presents the test procedure; experimental results are introduced in Section 6 and discussed in Section 7. Finally, conclusions are drawn in Section 8.

## 2. HEAVE MEASUREMENT BY IMU SENSORS

The heave can be defined as the vertical displacement along the vertical axis of the vessel. Heave measurement is required for various marine applications, such as hydrographic surveys, navigation, and sea operations. For example, when a crane lifts a load, precise heave information is required to manage the operation. In Active Heave Compensation (AHC) systems, an accurate estimate of the vertical vessel motion is needed to decouple the offshore crane's lift operation from the motion of the vessel [21]. In the present research plan, heave constitutes the key information for the sea state estimation and the proposed approach is based on IMU measurements.

A typical IMU is shown in Figure 1. It includes a triaxial accelerometer, a triaxial gyroscope and a triaxial magnetometer, plus auxiliary sensors, that are desirable to control influence environmental quantities. A sensor fusion algorithm is typically provided, to compensate for sensor metrological defects, such as offset and drift, to obtain the sensor orientation. To this purpose, in commercial devices, a proprietary sensor fusion filter is used, such as the Extended Kalman Filter (EKF) [22], [23]. Other options include complementary or the Madgwick filters [24],[25]. Filter properties are usually adapted through their parameters to each specific application, such as terrestrial navigation, marine or underwater navigation, human movement reconstruction, robotics, and so on.

The presence of a magnetometer is necessary to create a fixed reference system. The north direction is measured by the magnetometer, and together with the gravity direction as measured by the accelerometer, they create the fixed reference frame in which the orientation is measured. Unfortunately, the magnetometer and, consequently, the fixed reference system orientation suffer from magnetic disturbances. On-site magnetometer calibration procedures are provided by the manufacturers to characterize the magnetic field near the measurement position. This procedure can be three dimensional when it is possible to move the setup in three directions, bidimensional when only a planar movement is possible or based on a sort of auto-calibration that benefits from the sensor movements during normal operation.

The IMU's main output is its orientation, while raw sensors signal, such as accelerations, are available as output also. For a heave measurement, further processing is required to obtain the

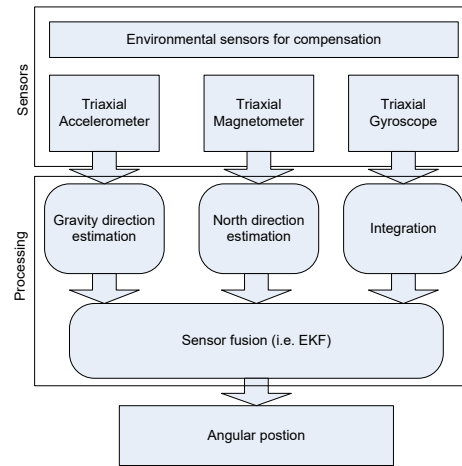


Figure 1. IMU functional scheme.

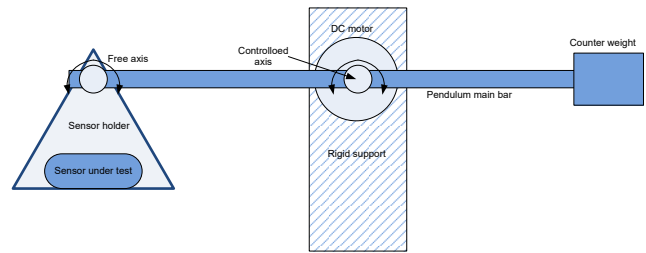


Figure 2. Functional scheme of the wave simulator.

displacement of the sensor along the vertical fixed axis. Some commercial, highly specialized sensors [22], [26]-[29] directly offer this output for marine applications. Such sensors are designed for buoy operation, and the processing algorithms directly provide a measurement of buoy displacements and sea wave parameters, such as wave period and direction. The necessary processing algorithms are proprietary and not publicly available. Thus, since the IMU considered for the current tests is a general one, further processing of the IMU outputs is necessary to obtain heave, as discussed in Section 4.

A general IMU sensor is focused on orientation measurements, as described in Figure 1, yet it also provides raw data from its sensors, particularly accelerations and the rate of turn in three dimensions. The double integration of the acceleration data can provide an estimation of the sensor's motion along each axis, but such an operation is not straightforward. In fact, a simple integration of these signals would result in a drifting signal due to typical sensor errors like noise, bias, drift, and misalignment [30]. A typical approach in heave measurements proposes a bandpass filter [31] with cut-off frequencies chosen in accordance with the current sea state. This approach requires continuous adaptation of the filters, which is complex to implement for application onboard a vessel. Moreover, since often the noise contribution at high frequencies on the displacement signal is rather low, a high-pass filter may be sufficient for drift removal [21]. In both high-pass or band-pass filtering cases, the fundamental problem is the selection of the best cutoff frequency [31].

In this paper, both high-pass and band-pass procedures are proposed. The intention was to have fixed cut-off frequencies to maintain a standard configuration, without the need for adaptation to sea conditions. For this reason, the frequency range considered must be rather large to include the most common sea conditions. In [32], both wind and swell sea conditions are

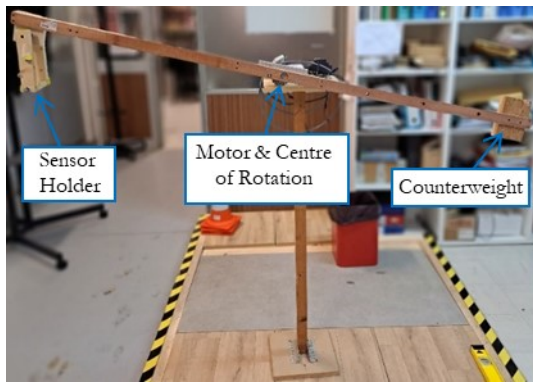


Figure 3. Pendulum setup.

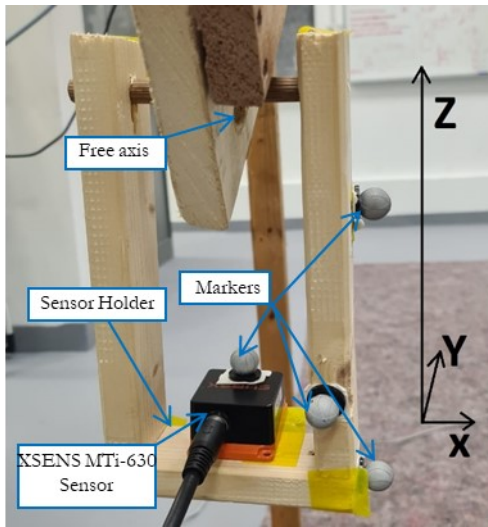


Figure 4. The sensor holder with XSENS MTi-630 equipped with the motion capture markers. The quantity of interest (heave) is in the Z direction.

analyzed, identifying the main spectral characteristics. Other papers [33] confirm that the range starts from frequencies down to 0.05 Hz (20 s period) up to around 1 Hz (1 s period). The important point is that the applied frequencies appear in the ocean, and they are in the scope of our research [34], [35]. This is also confirmed by commercial IMU-based wave sensor specifications; for example, in [22], the longest period measured is 15 s (0.067 Hz). Based on this, the filtering procedures implemented consider a band from 0.04 Hz up to 2 Hz in the case of band-pass filtering.

### 3. LABORATORY SETUP

#### 3.1. Wave simulator

To verify the potential of an IMU sensor for heave measurements, a dry wave simulator has been designed, following the approach used for buoy calibration [14]. Several possibilities were investigated and tested before arriving at the final setup.

The first attempt was a passive pendulum setup. This solution, although simple and easy to realize, presents some limitations. First, the amplitudes are not constant due to friction problems. Secondly, the wave period cannot be easily changed or controlled accurately.

An active solution could solve such problems, so a robotic arm was tested as a programmable wave generator. Unfortunately, magnetic disturbances were significant, making it

impossible to apply a calibration procedure. Moreover, the presence of large electric motors created variable magnetic interference that was difficult to compensate for without the GNSS signal, which was not available inside the laboratory.

Finally, a custom active pendulum was designed. The scheme in Figure 2 depicts its main characteristics. The device is primarily made of wood and aluminium, avoiding ferromagnetic materials near the sensor under test (Figure 3). The drive motor is placed in the centre, about 1 meter from the sensor, to minimize magnetic interferences.

At the wooden pendulum extremes, there are a movable sensor holder and a counterweight to balance the pendulum beam and reduce the motor's effort to move it. To better simulate the movement due to a sea wave, the sensor holder can move around the bar with a passive rotation joint. The internal properties of the sensor holder produce some oscillations around the horizontal position, creating a realistic movement very similar to the one present onboard a vessel.

The passive joint is realized using a wooden axle and plastic bearings. Finally, the sensor is placed on the holder as shown in Figure 4, using adhesive tape to avoid any magnetic interference.

The pendulum's main joint is actuated by a motor with an internal encoder, and the angular position is controlled in feedback through a Proportional Integral control by a personal computer. The control program manages a sinusoidal angular movement at variable frequency and amplitude. The corresponding vertical displacement of the sensor depends on both the mechanical assembly and the dynamics affecting the free oscillations of the sensor holder. This is not an issue since the external measurement system, described in the following paragraph, measures the sensor's movement externally.

#### 3.2. External optoelectronic reference system

The proposed verification procedure is based on an external measurement system considered as the reference standard. As already mentioned, this is a special aspect of this approach, since in the literature, the mechanical system is generally considered the reference itself.

The external reference is an optoelectronic system, based on eight infrared cameras by VICON®. The eight cameras - VICON VERO 2.2 - controlled by the NEXUS environment are uniformly distributed around the perimeter of a 5 m x 3 m room to measure the trajectories of four retroreflective markers on the sensor and its holder. Before starting the measurement campaign, the system was calibrated using the proprietary VICON device to achieve the declared accuracy below 1 mm [36]. Note that 1 mm accuracy is at least ten times the precision of a specialized heave sensor whose uncertainty is above 1 cm.

The four markers are placed on the sensor and on the sensor holder, which can be considered a rigid body. Their positions were optimized for the best camera view, with three markers placed laterally on the holder and one on the sensor, as shown in Figure 4. Marker trajectories during pendulum movements are reconstructed by VICON NEXUS software and are available as output at a 100 Hz sampling frequency. Further processing down-samples the reference trajectories to 10 Hz, the same as the IMU sampling frequency.

#### 3.3. IMU sensor under test

The sensor used in the experimentation is a Movella - XSENS model MTi-630. It is an IMU often used for Attitude Heading Reference System (AHRS) applications, with 10 Degrees of Freedom: 3D accelerometers, 3D gyroscopes, 3D

magnetometers, and a barometer. The sensor is specialized for orientation measurements in vehicles or vessels.

IMU internal sensors' specifications are reported in Table 1, Table 2, Table 3 and Table 4. The orientation measurement accuracy is presented in Table 5. In general, IMU units can be divided into classes when navigation is involved [37]. A navigation application requires very low angular drift (below  $0.05^\circ/\text{h}$ ). In this case, the sensor presents  $8^\circ/\text{h}$ , placing itself in the industrial grade.

Orientation data and raw sensor signal are available after each test at a 10 Hz sampling frequency.

#### 4. DATA PROCESSING

As mentioned in Section 1, heave can be obtained by double integration of the accelerometer signal in the vertical direction. A flow chart of the processing procedure is presented in Figure 5.

To obtain a displacement referred to the fixed, or world, reference system, common with the external reference instrument, the angular orientation of the IMU must be considered. Accelerometer signals are oriented along the moving sensor frame and must be rotated to be referred to the fixed reference frame. In this case, since the sensor is mounted on a free joint support, its orientation presents angular movements around the horizontal position due to the dynamics of the system. Figure 6 presents an example of acceleration rotation.

Then it is necessary to subtract from the vertical component the fixed contribution due to gravity to obtain the dynamic acceleration. Figure 7 presents the three dynamic acceleration components.

A first integration is carried out, as shown in Figure 8a. Although the gravity acceleration has been compensated, sensor offset, and offset drift are evident. Since, in this specific case, displacements due to a periodic motion at rather low frequencies are of primary interest, it is possible to process the velocity signal by high-pass filtering, as shown in Figure 8b. Considering the

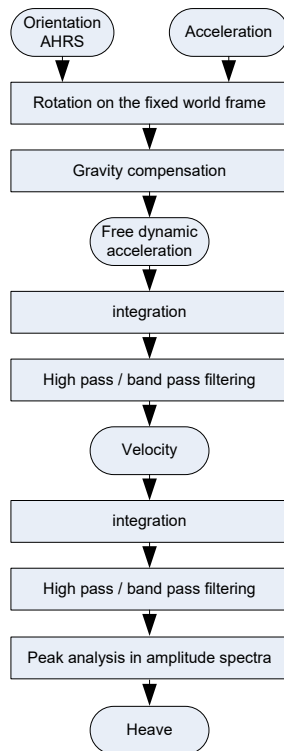


Figure 5. Scheme of the processing procedure.

Table 1. XSENS MTI-630 accelerometer metrological specifications [23].

Specifications	Unit	Value
Full range	$\text{m/s}^2$	$\pm 98.1$
In-run bias stability	$\text{m/s}^2$	$9.81 \times 10^{-5}$
In-run bias stability z	$\text{m/s}^2$	$1.471 \times 10^{-3}$
Bandwidth	Hz	500
Noise density	$\text{m}^2/\text{s}^4/\text{Hz}$	$3.4 \times 10^{-7}$
Non-linearity	%	0.1

Table 2. XSENS MTI-630 gyroscope metrological specifications [23].

Specifications	Unit	Value
Full range	$^\circ/\text{s}$	$\pm 2000$
In-run bias stability	$^\circ/\text{h}$	8
Bandwidth	Hz	520
Noise density	$(^\circ/\text{s})/\sqrt{\text{Hz}}$	0.007
Non-linearity	%	0.1

Table 3. XSENS MTI-630 magnetometer metrological specifications [23].

Specifications	Unit	Value
Full range	G	$\pm 8$
Non-linearity	%	0.2
Total RMS noise	mG	1
Resolution	mG	0.25

Table 4. XSENS MTI-630 barometer metrological specifications [23].

Specifications	Unit	Value
Full range	hPa	300-1250
Total RMS noise	Pa	1.2
Relative accuracy	Pa	$\pm 8$

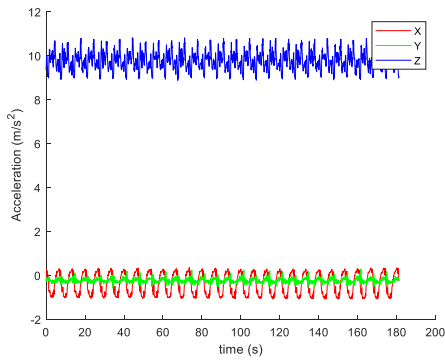
Table 5. XSENS MTI-630 orientation performance specifications [23].

Parameters	Performance	
	Static	Dynamic
Roll / Pitch	$0.2^\circ$	$0.25^\circ$
Yaw	NA	$1^\circ$

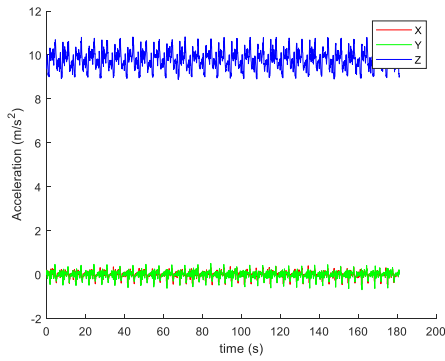
application, as described in Section 1, high-pass filtering is realized by a Butterworth 8th order filter, at a 0.04 Hz cutoff frequency.

The cut off frequency has been optimized to minimize the residual fluctuations in the frequency range considered for the heave movement.

Moreover, a bandpass Butterworth filter was considered to reduce any high-frequency noise contributions. In this case, the high-frequency cutoff was set at 2 Hz, while the low cutoff remained the same as before. Filtered velocity is then integrated to obtain displacement (Figure 9a). The same filtering procedure, with identical parameters, is then applied after the second integration, obtaining the curves shown in Figure 9b, using high-pass or bandpass filtering. Filter parameters have been adjusted to optimize the results, but since the intention was to provide a unique filtering for all sea conditions, or in this case, for all induced sensor motions, some fluctuations are still present (Figure 9b).



a)



b)

b

Figure 6. Acceleration measured along the sensor moving frame (a) and after rotation along the fixed reference frame (b).

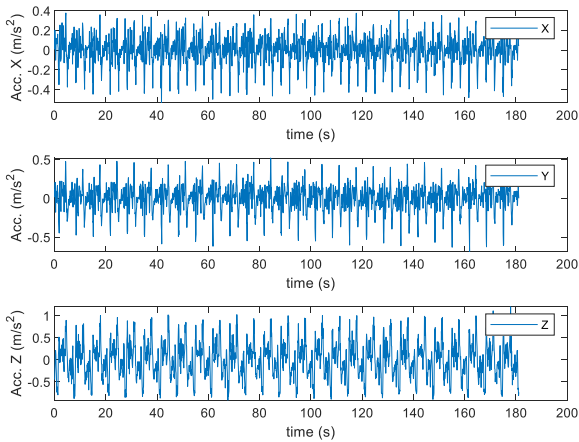
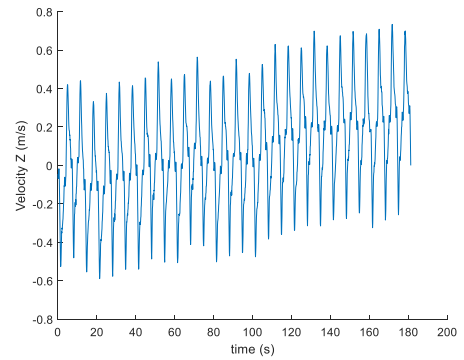


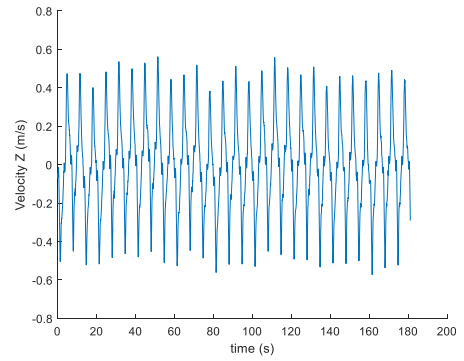
Figure 7. Dynamic accelerations in the fixed, world, reference frame.

In such conditions, it is difficult to obtain information about the periodic motion from displacement time history alone. A more robust approach is to consider the displacement signal spectra. For this reason, displacement signals from each trial have been analysed using a Fast Fourier Transform procedure, without any windowing on the time history, and introducing zero-padding equal to the first power of two larger than four times the points available in each trial.

Considering the amplitude spectra allows for a quantitative analysis by comparing the peak amplitudes of the reference and IMU heave signals and their absolute or relative differences. It is worth noting that the spectra will also present components due to residual fluctuations that are not eliminated by the filters. Such

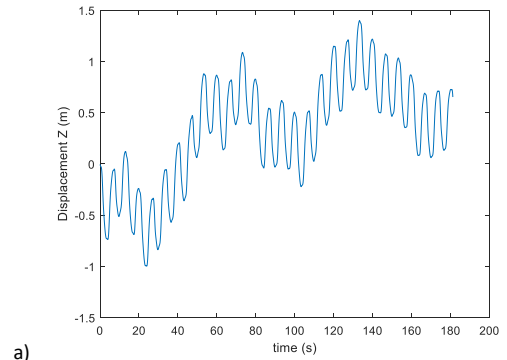


a)

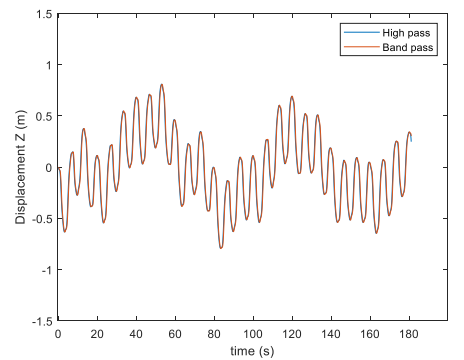


b)

Figure 8. Velocity obtained by integration before (a) and after high pass filtering (b).



a)



b)

Figure 9. Displacements obtained integrating the filtered velocity (a) and then using a 0.01 Hz high pass (b - blue) or 0.01 Hz – 2 Hz band pass filtering (b - red).

contributions are not considered in the comparison since they do not correspond to the maximum peak amplitude.

Table 6. Mean vertical displacement in meters for each angular amplitude measured by the optoelectronic with an uncertainty 1 mm [39].

A	B	C	D
1.483	1.264	0.889	0.607

Table 7. Test sequence and trial repetitions

Frequency (Hz)	Wave period (s)	Repetitions			
		A	B	C	D
0.05	20	3	5	3	5
0.10	10	3	5	3	5
0.15	6.7	3	5	3	5
0.20	5	5	5	5	5
0.25	4	3	5	3	5

## 5. TEST PROCEDURE

The pendulum carrying the IMU under test was moved inside the measurement volume of the optoelectronic measurement system, setting four different angular amplitudes for five different frequencies. Since the pendulum is controlled for its angular movement and not for the amplitude of the vertical sensor displacement, the four amplitude conditions are indicated by the letters A to D. Each letter corresponds to a mean vertical movement decreasing from A to D, as reported in Table 6. The displacement value for each trial is measured by the reference external instrument. The overall test sequence includes from 3 to 5 repetitions in each condition as reported in Table 7.

During normal sea operation the sensor will acquire continuously the wave movement, that usually presents a slow varying period so that it can be considered stationary. In the laboratory it is difficult to recreate stationary conditions, since the trials have a finite length and the processing of a huge amount of data from the optoelectronic system is rather time consuming. So, an optimal length was identified, which constitute a compromise between stationarity of the periodic movement and practical feasibility. A minimum of 20 wave periods is acquired in each trial so the longest acquisition reach 7 minutes.

During the tests, the reference measurement system and the IMU under test operates independently, so offline, before comparing results from the two system a synchronization is required (Figure 10a). Cross correlation was used to synchronize the two signals obtaining a couple of signals as shown in Figure 10b.

## 6. RESULTS

The heave signal in time is presented in Figure 11 for the frequencies tested at maximum amplitude (A in Table 6). As already introduced in Section 4, fluctuations are still evident after filtering. This is also evident in the amplitude spectra in Figure 12, but it is possible to clearly identify the main amplitude peak.

## 7. DISCUSSION

The results obtained with the proposed procedure can be considered from different points of view. The first regards the proposed calibration procedure, which enables a complete characterization of a sensor considering its dynamic behavior. Figure 13 and Figure 14 present the deviation of the sensor as a

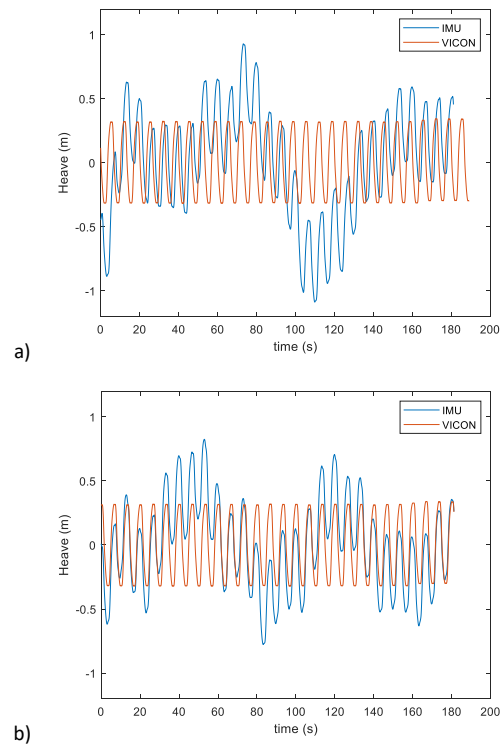


Figure 10. Vertical displacements obtained by Vicon and IMU before (a) and after (b) synchronization.

function of wave frequency and amplitude. Even though not strictly required, since the intention is to simulate real sensor movements due to vessel or buoy motion, the motion generated is almost sinusoidal with a maximum harmonic content of about 5% (see for example Figure 12a), with content at 0.3 Hz relative to the main component at 0.1 Hz. The amplitude range is limited to about 1.6 m due to limitations of the active pendulum device, which can be overcome if required by proper dimensional scaling of the mechanical setup. The frequency is limited at high frequencies by the dynamics of the system, but 0.25 Hz is already a rather high frequency for wave sensors. In the lower part of the spectrum, there is no limitation, although the slow motion or smoothness of the movement can be affected by the encoder resolution on the motor, which, if necessary, can be improved. Finally, in all testing conditions, independently from the mechanical performance of the motion device, the measurement uncertainty corresponds to the uncertainty of the optoelectronic reference instrument, certified at 1 mm [36].

Considering the performance of the sensor under test, the two filtering strategies considered give very similar results: their mean difference in heave measurement, considering all the testing conditions, is 3 mm. Their difference with the reference system has the same standard deviation. So, for the device under test, the noise contribution on the heave measurement can be considered negligible.

Looking at the time signal (Figure 11) there are signal fluctuations that both the procedures are not able to avoid. Such residual behavior could be eliminated by adapting properly, case by case, the filters low frequency cut; however, since the interest here is to measurement the wave heave in all possible sea conditions, the low frequency cut must be fixed for all the tests at a reasonable frequency considering the motion of interest. After some test the low cut was fixed at 0.04 Hz, to be able to measure the wave motion down to 0.05 Hz.

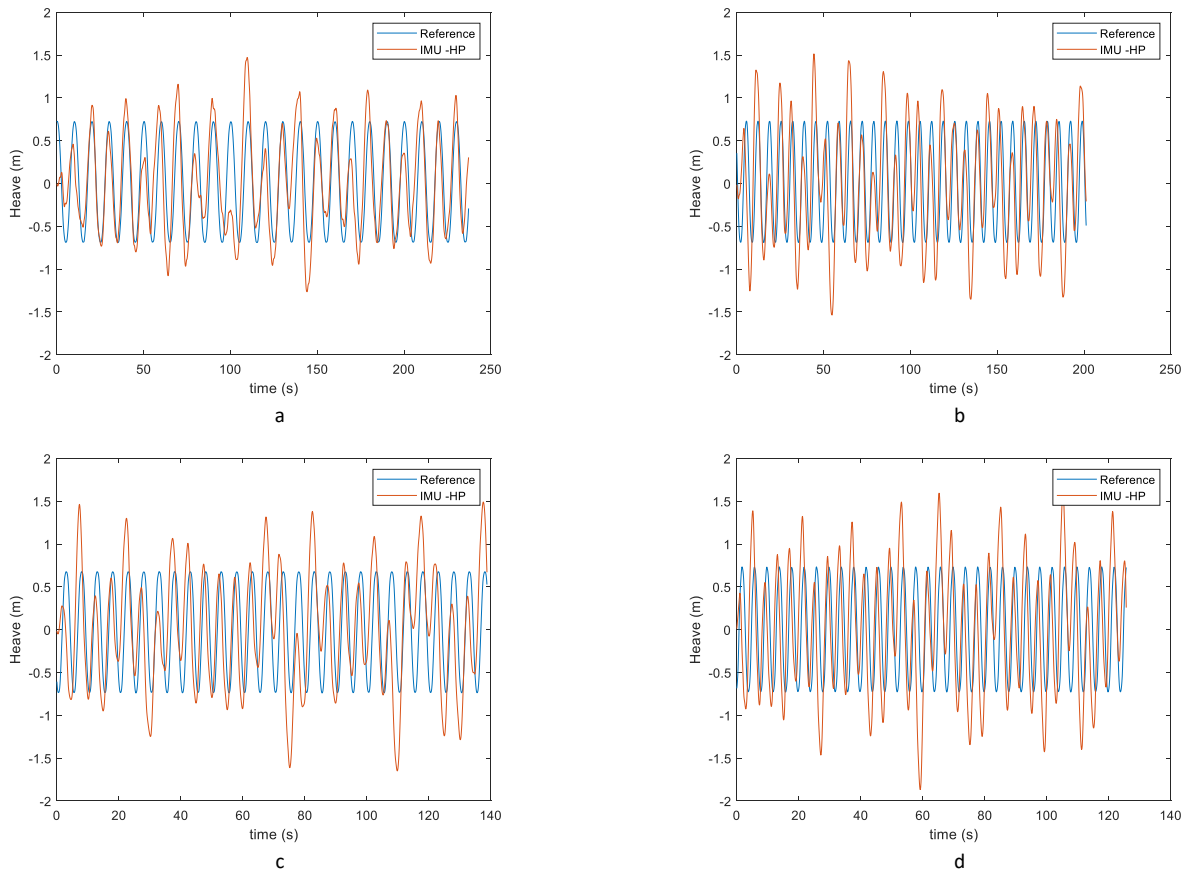


Figure 11. Example of heave time histories at maximum amplitude for frequencies 0.10 Hz (a), 0.15 Hz (b), 0.20 Hz (c), 0.25 Hz (d). The reference heave signal is presented in blue the high pass filtered IMU signal in red.

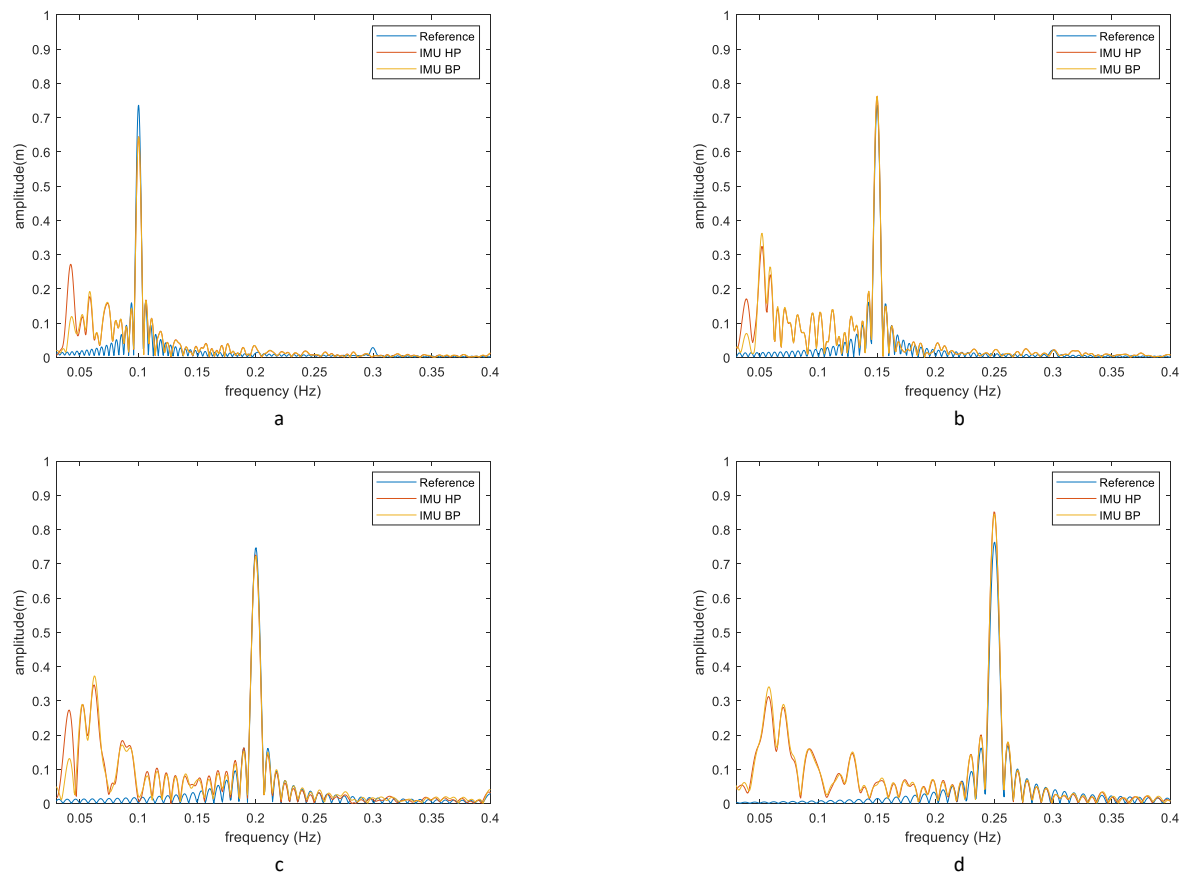


Figure 12. Example of heave spectra at maximum amplitude for frequencies 0.1 Hz (a), 0.15 Hz (b), 0.20 Hz (c), 0.25 Hz (d). The three lines represent the reference signal (blue), the IMU heave obtained by high pass filtering (red), the same obtained by band pass filtering (orange).



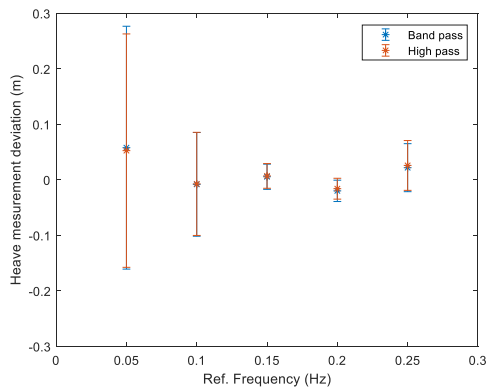


Figure 13. IMU heave measurement deviation as a function of reference frequency for all the amplitudes. Bars indicate one standard deviation.

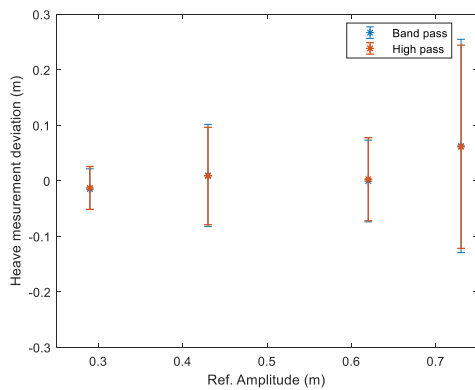


Figure 14. IMU heave measurement deviation as a function of reference amplitude for all the frequencies. Bars indicate one standard deviation.

More in detail, Figure 13 and Figure 14 present the deviation in the heave measurement as a function of amplitude and frequency for the two filtering procedures, with its standard deviation. The overall deviation mean value of 20 mm and standard deviation of about 110 mm is affected by the large deviation at the lowest frequency of 0.05 Hz. The repeatability, computed as the standard deviation in the same test conditions, in average is 25 mm, excluding the lowest frequency, for which it ranges from 32 to 220 mm, demonstrating the instability of the heave measurements at 0.05 Hz. In general, typical uncertainty values for commercial devices specialized for heave and wave period measurements varies from sensor to another, the best heave measurement accuracy of about 30 mm or 3 %, is obtained by the very expensive fiberoptic sensors [38]. For a MEMS based sensor, the accuracy varies depending on if it is integrated with GNSS receiver or not. The accuracy of an IMU integrated with GNSS receiver is 50 mm or 5 %, while if it is not integrated it is 100 mm or 10 % [39]. The sensor under test shows an offset that should not be present and a standard deviation far above a specialized sensor. If the trials carried out at the lowest frequency 0.05 Hz are excluded from the evaluation, the situation improves, obtaining an overall mean offset of about 1 mm and a standard deviation of 53 mm. Considering that the reference instrument has a measurement uncertainty of 1 mm, the heave measurement standard uncertainty in such general conditions can be evaluated in 53 mm including the contribution of repeatability. So, in a reduced operating range, the sensor under test has a reasonable performance as compared with a specialized sensor.

Excluding the lowest frequency, at 0.05 Hz, the measurement deviation does not present an evident dependence on frequency

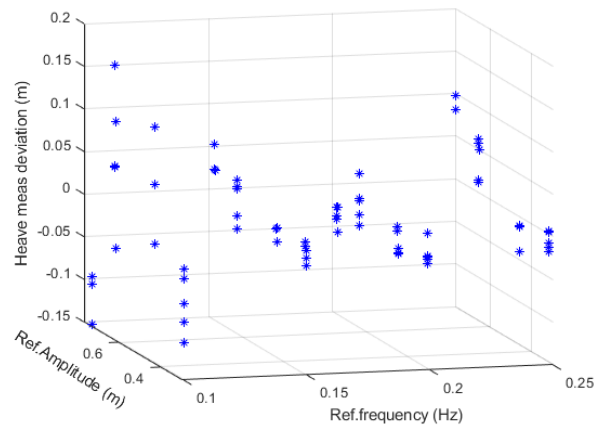


Figure 15. Heave measurement deviation for band pass filtering as a function of amplitude and frequency, excluding the lowest one, 0.05 Hz.

or amplitude, as shown in Figure 15. This confirms that the couple sensor and filtering procedure has the proper bandwidth for a sea wave measurement, and that its linearity is confirmed in the range of amplitudes tested, between 1.4 m and 0.6 m.

## 8. CONCLUSIONS

The proposed procedure based on an active motor-driven pendulum, operating in the volume of an optoelectronic measurement system used as a reference, demonstrated to be effective for IMU based heave measurement calibration.

The possibility to control the device enables verifications in both frequency and amplitudes for a complete sensor characterization.

The experimental campaign was focused on a standard IMU not specifically designed for heave measurements, so it was necessary to setup and validate the processing procedure to obtain the heave information also. Consequently, the experimental trials not only were useful to validate the calibration procedure but also to verify the reliability of the proposed approach to the heave measurement from the raw accelerometric IMU signals.

Since in the real application the sensor will continuously measure the heave motion, in future the effect of the time history length will be investigated, to understand how the number of measured oscillations affect the result. Such information will be interesting for real time applications on variable sea state conditions. Further developments will regard the application of the same procedure to the verification of wave motion specialized IMU sensors. Furthermore, as secondary result from these tests, thanks to the external reference instrument, it will be possible to characterize the mechanical device to obtain its mechanics uncertainty in the movement generation. After that it will be possible to use it as a secondary standard for example to calibrate sensors outdoor without the reference optoelectronic system. Such application will be particularly interesting for the verification of GNSS based sensors.

## ACKNOWLEDGEMENT

Partially funded by the European Union – Next Generation EU and by the Ministry of University and Research (MUR), National Recovery and Resilience Plan (NRRP), Mission 4, Component 2, Investment 1.5, project “RAISE - Robotics and AI for Socio-economic Empowerment” (ECS00000035).

## REFERENCES

- [1] G. B. Rossi, A. Cannata, A. Iengo, M. Migliaccio, G. Nardone, V. Piscopo, E. Zambianchi, Measurement of sea waves, *Sensors* 22(1) (2022), art. No. 78.  
DOI: [10.3390/s22010078](https://doi.org/10.3390/s22010078)
- [2] M. Berardengo, G. B. Rossi, F. Crenna, Sea spectral estimation using arma models, *Sensors* 21(13) (2021), art. No. 4280.  
DOI: [10.3390/s21134280](https://doi.org/10.3390/s21134280)
- [3] U. D. Nielsen, A concise account of techniques available for shipboard sea state estimation, *Ocean Engineering* 129 (2017), pp. 352-362.  
DOI: [10.1016/j.oceaneng.2016.11.035](https://doi.org/10.1016/j.oceaneng.2016.11.035)
- [4] R. Pascoal, C. G. Soares, Kalman filtering of vessel motions for ocean wave directional spectrum estimation, *Ocean Engineering* 36 (2009), pp. 477-488.  
DOI: [10.1016/j.oceaneng.2009.01.013](https://doi.org/10.1016/j.oceaneng.2009.01.013)
- [5] U. D. Nielsen, Transformation of a wave energy spectrum from encounter to absolute domain when observing from an advancing ship, *Applied Ocean Research* 69 (2017), pp. 160-172.  
DOI: [10.1016/j.apor.2017.10.011](https://doi.org/10.1016/j.apor.2017.10.011)
- [6] U. D. Nielsen, J. Dietz, Ocean wave spectrum estimation using measured vessel motions from an in-service container ship, *Marine Structures* 69 (2020), art. no. 102682.  
DOI: [10.1016/j.marstruc.2019.102682](https://doi.org/10.1016/j.marstruc.2019.102682)
- [7] Y. Y. Yurovsky, V. A. Dulov, MEMS-based wave buoy: Towards short wind-wave sensing, *Ocean Engineering* 217 (2020), art. No. 108043.  
DOI: [10.1016/j.oceaneng.2020.108043](https://doi.org/10.1016/j.oceaneng.2020.108043)
- [8] J. K. Woodacre, R. J. Bauer, R. A. Irani, A review of vertical motion heave compensation systems, *Ocean Engineering* 104 (2015), pp. 140-154.  
DOI: [10.1016/j.oceaneng.2015.05.004](https://doi.org/10.1016/j.oceaneng.2015.05.004)
- [9] J. V. P. Rapatz, Vessel heave determination using the Global Positioning System, (2023). Online [Accessed 12 August 2024]  
<https://unbscholar.lib.unb.ca/handle/1882/33795>
- [10] G. B. Rossi, F. Crenna, A. Palazzo, A proposal for a more user-oriented GUM, *IEEE Transactions on Instrumentation and Measurement* 68 (2019) pp. 1343-1352.  
DOI: [10.1109/TIM.2019.2899183](https://doi.org/10.1109/TIM.2019.2899183)
- [11] C. V. Amaechi, F. Wang, J. Ye, Experimental study on motion characterisation of CALM buoy hose system under water waves, *Journal of Marine Science and Engineering* 10(2) (2022), art. no. 204.  
DOI: [10.3390/jmse10020204](https://doi.org/10.3390/jmse10020204)
- [12] D. F. Gunn, M. Rudman, R. C. Z. Cohen, Wave interaction with a tethered buoy: SPH simulation and experimental validation, *Ocean Engineering* 156 (2018), pp. 306-317.  
DOI: [10.1016/j.oceaneng.2018.03.001](https://doi.org/10.1016/j.oceaneng.2018.03.001)
- [13] Datawell oceanographic instruments. Online [Accessed 12 August 2024].  
<http://www.datawell.nl>
- [14] P. L. Gerritzen, The calibration of wave buoys, *Calibration of Hydrographic Instrumentation*, Special Publication 31 (1993). Online [Accessed 12 August 2024].  
[https://datawell.nl/wp-content/uploads/2022/08/datawell\\_publication\\_hydrographicinstrumentation-calibrationwavebuoys.pdf](https://datawell.nl/wp-content/uploads/2022/08/datawell_publication_hydrographicinstrumentation-calibrationwavebuoys.pdf)
- [15] Y. Jianqing, How we calibrate the wave height and period measurements from the gravitational acceleration wave buoys in RMIC/AP, RMIC for the Asia-Pacific Region National Center of Ocean Standards and Metrology, China (2014).
- [16] D. G. Gryazin, Providing waverider buoys with metrological data. *Problems and Solutions*, *Physical Oceanography* 25 (2018), pp. 144-152.  
DOI: [10.22449/1573-160X-2018-2-144-152](https://doi.org/10.22449/1573-160X-2018-2-144-152)
- [17] M. Marin-Perianu, S. Chatterjea, R. Marin-Perianu, S. Bosch, S. Dulman, S. Kininmonth, P. Havinga, Wave monitoring with wireless sensor networks, *Proc. of 2008 IEEE Int. Conf. on Intelligent Sensors, Sensor Networks and Information Processing*, Sydney, NSW, Australia, 15-18 December 2008.  
DOI: [10.1109/ISSNIP.2008.4762057](https://doi.org/10.1109/ISSNIP.2008.4762057)
- [18] J. J. De Vries, J. Waldron, V. Cunningham, Field tests of the new Datawell DWR-G GPA wave buoy, *Sea Technology* 44 (2003) pp. 50-55. Online [Accessed 12 August 2024]  
[https://datawell.nl/wp-content/uploads/2022/08/datawell\\_publication\\_dwr-g\\_seatechnology.pdf](https://datawell.nl/wp-content/uploads/2022/08/datawell_publication_dwr-g_seatechnology.pdf)
- [19] D.-J. Doong, B.-C. Lee, C. C. Kao, Wave measurements using GPS velocity signals, *Sensors* 11(1) (2011), pp. 1043-1058.  
DOI: [10.3390/s110101043](https://doi.org/10.3390/s110101043)
- [20] G. Joodaki, H. Nahavandchi, K. Cheng, Ocean wave measurement using GPS buoys, *Journal of Geodetic Science* 3 (2013), pp. 163-172.  
DOI: [10.2478/jogs-2013-0023](https://doi.org/10.2478/jogs-2013-0023)
- [21] M. Richter, K. Schneider, D. Walser, O. Sawodny, Real-time heave motion estimation using adaptive filtering techniques, *IFAC Proceedings Volumes* 47(3) (2014), pp. 10119-10125.  
DOI: [10.3182/20140824-6-ZA-1003.00111](https://doi.org/10.3182/20140824-6-ZA-1003.00111)
- [22] SBG Systems. Online [Accessed 12 August 2024]  
<https://www.sbg-systems.com>
- [23] Movella. Online [Accessed 12 August 2024]  
<https://www.movella.com>
- [24] M. Euston, P. Coote, R. Mahony, J. Kim, T. Hamel, A complementary filter for attitude estimation of a fixed-wing UAV, 2008 IEEE/RSJ International Conference on Intelligent Robots and Systems, Nice, France, 22-26 September 2008.  
DOI: [10.1109/IROS.2008.4650766](https://doi.org/10.1109/IROS.2008.4650766)
- [25] J. Justa, V. Šmídl, A. Hamáček, Fast AHRS filter for accelerometer, magnetometer, and gyroscope combination with separated sensor corrections, *Sensors* 20 (2020) pp. 3824.
- [26] Advanced Navigation. Online [Accessed 12 August 2024]  
<https://www.advancednavigation.com>
- [27] Inertial Labs. Online [Accessed 12 August 2024]  
<https://www.inertiallabs.com>
- [28] VECTORNAV. Online [Accessed 12 August 2024]  
<https://www.vectornav.com>
- [29] KONGSBERG. Online [Accessed 12 August 2024]  
<https://www.kongsberg.com>
- [30] S. Küchler, J.K. Eberharter, K. Langer, K. Schneider, O. Sawodny, Heave motion estimation of a vessel using acceleration measurements, *IFAC Proceedings* 44(1) (2011) pp. 14742-14747.  
DOI: [10.3182/20110828-6-IT-1002.01935](https://doi.org/10.3182/20110828-6-IT-1002.01935)
- [31] J.-M. Godhaven, Adaptive tuning of heave filter in motion sensor, in *IEEE Oceanic Engineering Society. OCEANS'98. Conference Proceedings (Cat. No.98CH36259) Proceedings*, Nice, France, 28 September 1998 - 01 October 1998, pp. 14742-14747.  
DOI: [10.1109/OCEANS.1998.725731](https://doi.org/10.1109/OCEANS.1998.725731)
- [32] V. Piscopo, A. Scamardella, S. Gaglione, A new wave spectrum resembling procedure based on ship motion analysis, *Ocean Engineering* 201 (2020), art. no. 107137.  
DOI: [10.1016/j.oceaneng.2020.107137](https://doi.org/10.1016/j.oceaneng.2020.107137)
- [33] J. Li, L. Li, X. Wen, A novel method of estimating ship heave motion based on dual inertial measurement units, *Journal of Physics: Conference Series* 2183 (2022).  
DOI: [10.1088/1742-6596/2183/1/012002](https://doi.org/10.1088/1742-6596/2183/1/012002)
- [34] W. H. Munk, *Origin and generation of waves*, Scripps Institution of Oceanography, La Jolla, California, 1951.
- [35] B. Kinsman, *Wind waves: their generation and propagation on the ocean surface*, Courier Corporation, 1984.
- [36] VICON. Online [Accessed 12 August 2024]  
<https://www.vicon.com>
- [37] INERTIALSENS. Online [Accessed 12 August 2024].  
<https://inertialsense.com>
- [38] Inertial Labs Datasheet. Online [Accessed 12 August 2024]  
<https://inertiallabs.com/mru-pd-datasheet>
- [39] SBG Systems Documentations. Online [Accessed 12 August 2024].  
<https://support.sbg-systems.com/sc/el/latest/documentations-resources/ellipse-documentation>